Electron field emission from room temperature grown carbon nanofibers

R. C. Smith,[a] J. D. Carey, C. H. P. Poa, D. C. Cox, and S. R. P. Silva
Advanced Technology Institute, School of Electronics and Physical Sciences University of Surrey, Guildford, Surrey, GU2 7XH, United Kingdom

(Received 21 October 2003; accepted 17 December 2003)

The observation of field induced electron emission from room temperature grown carbon nanofibers at low (5 V/μm) macroscopic electric fields is reported. The nanofibers were deposited using methane as a source gas in a conventional rf plasma enhanced chemical vapor deposition reactor using a Ni metal catalyst previously subjected to an Ar plasma treatment. Analysis of the scanning electron microscopy images of the nanofibers show them to possess an average diameter of 300 nm and that the nanofibers are observed to be radially dispersed over an area of 50 μm in diameter. No evidence of hysteresis in the current-voltage characteristic or conditioning of the emitters is observed. The mechanism for emission at low fields is attributed to field enhancement at the tips rather than from the surrounding amorphous carbon film which is shown to have a higher threshold field (20 V/μm) for emission. [DOI: 10.1063/1.1647261]

I. INTRODUCTION

Since the identification of carbon nanotubes (CNTs)[1] in 1991, there has been considerable interest in their field emission (FE) properties with the observation of electron emission at low macroscopic electric fields.[2] The ease of deposition over large areas has encouraged the belief that field emission displays (FEDs) utilizing carbon nanotubes as emitters can be an alternative technology for the next generation of flat panel displays based upon an emissive technology.[3] A suitable emissive display technology should be capable of high quality images with good color saturation and for large screen diagonals should be capable of competing with active matrix liquid crystal displays and plasma displays.[3] It has been shown that CNTs can now be readily deposited over substrate areas only limited by the size of deposition reactor. Such nanotip based emitters possess a distinct advantage over FED technologies, based on Spindt tips, which require more complex fabrication lithography and processing. While electron emission is possible from a single nanotube, for practical applications requiring suitable current densities, films or mats consisting of bundles of tubes are often employed.[4] In the high current density regime, CNTs also have the added advantage that they are less susceptible to the current induced electromigration of atoms due to the nature of the covalent bonding present. In addition to electron emission from CNTs, it is further possible to observe electron emission from CNTs embedded in polymer composite matrices[5] where the presence of the polymer provides addition mechanical support for the tubes as well as a way of tailoring the mass fraction of the nanotubes in their distribution.

Electron field emission from nanotip materials is not just confined to CNTs, but has been observed from a wide variety of material systems such as SiC nanowires,[6] MoO_3 nanobelts,[7] tungsten nanowires,[8] and copper sulphide nanowire arrays.[9] These studies demonstrate that considerable effort is being placed into developing alternative nanotip based emitter materials.

In this regard, the recent report of the growth of carbon nanofibers (CNFs) at room temperature[10] is significant and opens up the possibility of the growth at *low temperatures* of a cold cathode emitter material. These CNFs reported in Ref. 10 also have the added advantage of being deposited using the standard and mature technique of rf plasma enhanced chemical vapor deposition (PECVD). Growth at low temperatures using PECVD allows the potential use of plastic[11] or organic substrates and as a consequence, the choice and treatment applied to the substrates is an important consideration. It is generally agreed that for CNTs grown using Ni catalysts, the size and distribution of the Ni, usually in the form of islands, can determine the average diameter of the resultant tubes.[12] Thermal annealing of thin metal layers of transition metals to form nanostructured surfaces is the most common way to form Co islands[13] or Ni islands[14]—the latter study concentrating on low temperature ($<500\,^{\circ}C$) island formation. In this article, we report on the field emission characteristics of the room temperature deposited carbon nanofibers. A correlation between the FE characteristics and the structure of the material is presented and demonstrate that CNFs may be an alternative flat cathode material for large area FEDs. We also discuss the possible use of Ar ion treatment on thin Ni metal films as an alternative method to produce a nanostructured surface. Plasma treatment of a catalyst surface has the advantage that it may be carried out a low macroscopic temperatures thereby avoiding the need for high temperature processing and the ability to employ glass as substrates.

II. EXPERIMENTAL METHOD

Glass slide substrates were cleaned using a standard three stage chemical bath process on to which a 0.5 μm layer of Ni was thermally evaporated in a vacuum of 2×10^{-6} Torr. The Ni film was subsequently treated to an Ar

[a]Electronic mail: r.c.smith@eim.surrey.ac.uk

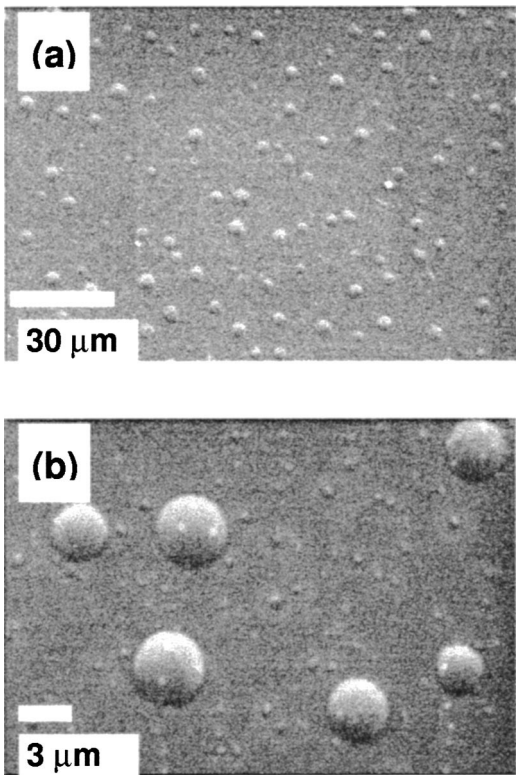

FIG. 1. (a) Scanning electron microscope image of the Ni film after Ar^+ treatment. A roughening of the film surface was observed with the formation of 3 μm circular features. (b) Higher magnification image of that of part (a), smaller circular feature of diameter ~500 nm are observed surrounding the larger features.

ion plasma of 100 sccm for 30 min at room temperature in a Plasma Technology DP800 capacitively coupled rf PECVD reaction chamber. A process pressure of 200 mTorr and a rf power of 300 W was used. The surface of the catalyst and the subsequent film was examined using a Hitachi S4000 cold field emission scanning electron microscope (SEM). The field emission characteristics of the CNFs were examined using a sphere-to-plane electrode geometry with a 5 mm stainless steel ball bearing suspended 30 μm above the sample with a high positive potential applied in a vacuum of around 10^{-6} Torr. Although a spherical anode is used it is assumed that the electric field between the anode and the surface of the sample can be modeled as a parallel plate. The voltage is stepped up and down four times in 20 V increments and the macroscopic electric field is defined as the applied voltage divided by the anode-cathode separation. Further details about the experimental setup can be found elsewhere.[15] The threshold field E_{th} is defined as the macroscopic electric field, which gives an emission current of 1 nA.

III. NANOFIBER GROWTH

The Ar plasma treatment of the Ni film produces a roughening of the film surface as shown by the circular features of Fig. 1(a). These features are of approximately 3 μm in diameter and are surrounded by smaller circular islands of less than 500 nm in diameter, as can be observed in the higher magnification image presented in Fig. 1(b). It is known from extensive studies of noble gas ion implantation that ''bubbles'' may form at sufficiently high dose and ion energies.[16] For example, 10^{17} Ar ions cm^{-2} irradiated into a copper foil at 60 keV ion energy at 20 °C showed the formation of bubbles.[16] In these studies, the bubbles are believed to consist of gas molecules which can burst and result in blisters. However, the energies of the Ar ions used in this study would be tens of electron volts not keV and as a result we do not believe that the features observed are bubbles of gas but rather are Ni metal. The formation of the Ni is most likely due to thermal processing experienced by the film via a form of plasma etching though the role of adhesion of the metal to the substrate may also be a contributory factor. It is interesting to note that in the growth of CNTs on plastic substrates, the formation of Ni islands was also attributed to plasma processing rather than adhesion.[11]

Nanofiber growth was then performed in the same reactor chamber, in which the sole deposition gas of CH_4 was introduced at a flow rate of 30 sccm and a pressure of 1 Torr. The reverse power of the plasma was continually adjusted to keep it as close to zero as possible in order to prevent substantial substrate heating. The water cooled substrate table temperature was monitored to be about 30 °C throughout the deposition. Both the Ar ion treatment and nanofiber growth were carried out on substrates held on the earthed electrode. It has been previously shown that depositing from a hydrocarbon gas in this reactor can readily lead to the formation of disordered amorphous carbon thin films.[17]

A SEM image of the surface after CH_4 deposition shows the growth structure of the nanofibers, arranged radially in clusters forming star shaped objects, approximately 50 μm across as shown in Fig. 2(a). The nanofibers are predominantly lying on the surface rather than vertically aligned. Toward the center of the cluster a higher concentration of fibers where diameters of 100–400 nm can be seen. Such structures are referred to here as carbon nanofibers rather than the related CNTs which often possess smaller diameters. The carbon nanofibers are observed to have well defined features including a rounded tip and a cylindrical shape as evidenced from a high resolution SEM of a group of nanofibers on the outside edge of the star structure shown in Fig. 2(a). [Due to the tilt of the sample when the SEM analysis was carried out and the fact that the emissive electrons are analogous to light, we see light and dark regions of the encircled fiber of Fig. 2(b), confirming a three-dimensional cylindrical shape.] At low growth temperatures, the diffusion of C in Ni is dominated by surface diffusion of C around Ni particles as opposed to C diffusion through the bulk of the metal.[10,11] The growth mechanism is based on the decomposition and diffusion of carbon through the Ni, similar to that described previously elsewhere in the low temperature growth of nanofibers.[10] At sufficient high C concentration precipitation of the C occurs above the solubility limit resulting in nanofibers growth. No evidence of Ni is seen in the high resolution electron microscope images and we conclude that in this case the growth mechanism is not by the usual ''tip growth'' mode. We believe the large scale Ni islands remain strongly adhered to the surface resulting in base growth mode. Indeed, for efficient Ni incorporation, it is necessary to lift the

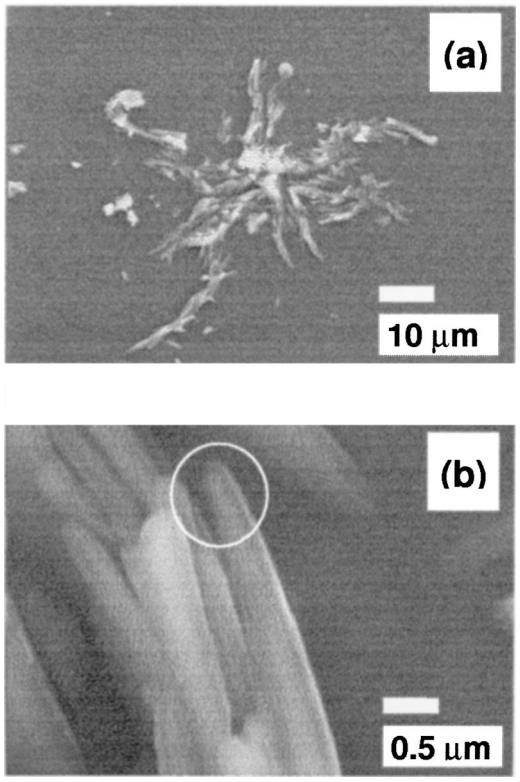

FIG. 2. (a) SEM image of nanofibers grown at room temperature by plasma enhanced chemical vapor deposition. The structures grow out from a central point to form star shapes consisting of many fibers. (b) Higher magnification SEM image of a group of nanofibers, orientated with each other. The nanofibers have a diameter of about 300 nm with rounded tips.

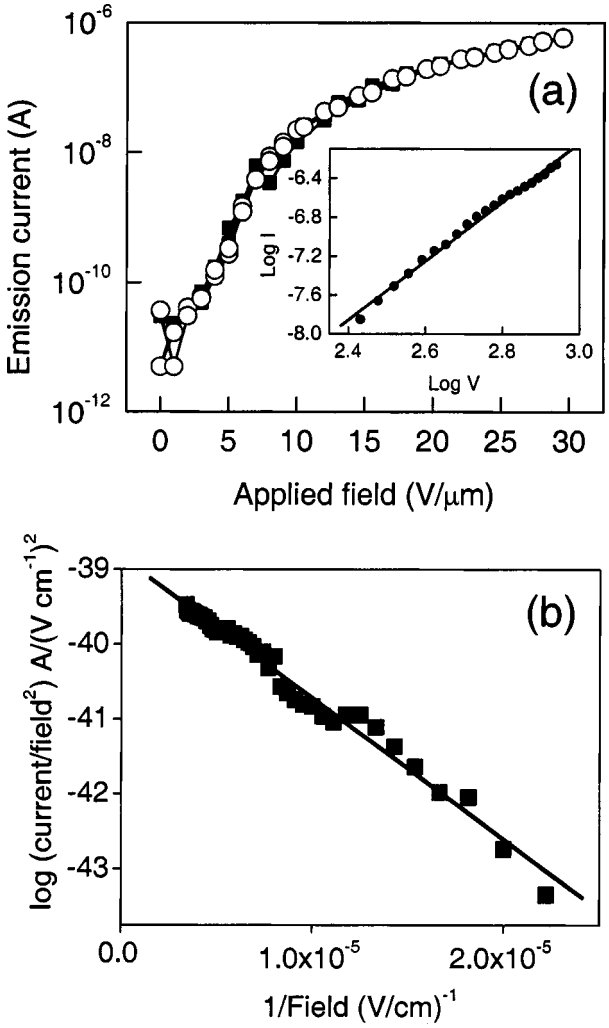

FIG. 3. (a) First (○) and second (■) field emission $I-E$ characteristics for the nanofiber sample. The threshold field (for 1 nA) can be seen as 5 V/μm. Inset: The fit in the high current regime to the $I-V$ characteristic assuming $I \propto V^n$ with $n=3.0$. (b) Fowler–Nordheim analysis of the field emission $I-E$ data of that of the first upward cycle of the voltage (field) from part (a). Note: not every data point has been plotted for the sake of clarity.

Ni particle from the substrate—an effect that tends to be enhanced for (i) Ni particles with nanometer sized diameters and (ii) on substrates that do not have strong interactions with the metal. This tends to be the case for certain classes of Ni films found in certain types of oxide whereby thermal annealing results in nm sized metal islands.[14] In addition, Merkulov and co-workers showed that it is possible for more than one nanotube to grow from a single Ni droplet if the diameter is sufficiently large.[18]

IV. FIELD EMISSION CHARACTERISTICS

The sample deposited at room temperature displayed excellent emission characteristics with a threshold field of 5 V/μm as shown in Fig. 3(a). The first two current-voltage characteristics are presented and no significant difference between the two $I-E$ characteristics is apparent. Further voltage cycles show the same behavior and implies that there is no need for a ''conditioning'' phase required for the onset of stable and reproducible emission. This is in contrast to what has been reported in some rf PECVD amorphous carbon (a-C) thin films.[15] In addition, there is no evidence of hysteresis behavior between the upward and downward cycle of either $I-E$ characteristic. This is an important result since any spread in the $I-E$ characteristic could mean more complicated and expensive drive circuitry for a nanofiber based field emission display.

To exclude the possibility of emission from the roughened Ni film substrate, the emission characteristics prior to CH_4 deposition were also tested. The results of the measurements [Fig. 4(a)] revealed only background noise (<50 pA) up to applied fields of 38 V/μm. This confirms the emission observed in Fig. 3(a) is due to the carbon growth stage. Furthermore, to confirm that the observed emission is from the CNFs rather than the surrounding amorphous carbon film, the FE characteristics of an area on the same sample that did not possess CNFs was tested by moving the probe anode. The FE results, presented in Fig. 4(b), show the difference in field emission characteristics from that of Fig. 3(a). First, the threshold field for this part of the sample can be seen to be approximately 20 V/μm, higher than reported previously and has a peak emission current of 10^{-8} A, lower than the peak current of 10^{-6} A seen in Fig. 3(a). Second, it is apparent there is a definite hysteresis between the upward and downward cycle of the electric fields consistent with conditioning cycles, as discussed previously. From these results we believe that the FE reported in Fig. 3(a) conclusively comes from the CNFs themselves.

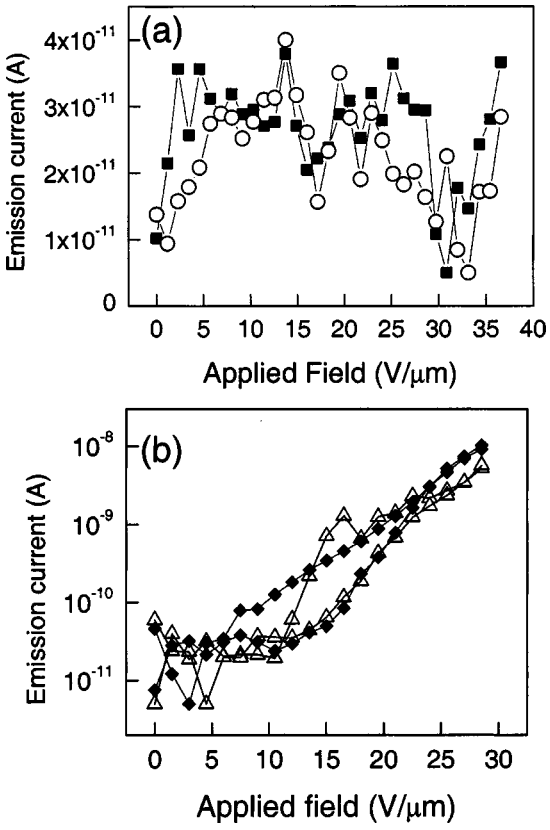

FIG. 4. (a) First (■) and second (○) voltage cycle of the Ni evaporated film. Note the current is pA. (b) First (△) and second (◆) field emission characteristics for the surrounding amorphous carbon area where hysteresis can be seen in both curves. The threshold field can be seen as 20 V/μm. Note: not every data point has been plotted for the sake of clarity.

In order to further explore the origins of the electron emission characteristics an analysis of the electron field emission $I-E$ characteristics presented in Fig. 3(a) was performed using the standard Fowler–Nordheim (FN) equation given by

$$I=\frac{aA\beta^2E^2}{\Phi}\exp\left(\frac{-b\Phi^{3/2}}{\beta E}\right), \tag{1}$$

where a and b are constants, having the values $1.54\times10^{-6}\,\mathrm{A\,eV\,V^{-2}}$ and $6.83\times10^{7}\,\mathrm{eV^{-3/2}\,V\,cm^{-1}}$, respectively. Variable A represents the emission area, Φ is the emission barrier and βE represents the *local* electric field. In this context β represents the field enhancement factor and Fig. 3(a) shows the $I-E$ characteristic of the first (upward) field cycle plotted in the usual FN coordinates.[19] The slope of the line is $-b\Phi^{3/2}/\beta$ and for a work function (barrier height) of 5 eV, a value of 4180 is found for the field enhancement factor β. Large values of enhancement factor have been reported previously from field emission measurements made over large areas rather than from individual tubes. For example, Bonard *et al.* reported that a field enhancement factor of 1800 was inferred from a large area measurement (1.88 cm^2 with an anode-cathode separation of 500 μm) whereas for single tubes, a value of β of only 230 was reported.[20] In another study, field enhancement factors of several thousand were also report by Bonard *et al.* from a film of single wall CNTs, however, no current saturation in the high current regime was reported in that study[21] unlike in the present case.

Some caution must be exercised in the FN analysis of the $I-E$ characteristic of Fig. 3(a) since there will be a distribution of field enhancement factors due to the different local workfunctions, a distribution in nanofiber lengths, radii, and screening due to proximity effects. In addition, a large value of enhancement factor can be inferred in the presence of a shallow $I-E$ characteristic due to a bulk transport limited emission behavior.[22] In this case, despite the apparent linearity of the FN plot, the presence of a bulk limited transport emission process complicates the use of the Fowler–Nordheim analysis. The possibility of bulk limited conduction was not considered in the original formulation of the Fowler–Nordheim theory of emission from metals due to high conductivity of the cathode. From Fig. 2(b), we can estimate the radius of curvature r of the emitter to be about 100 nm and from an enhancement factor of approximately 4200, would suggest an emitting structure of height h, 420 μm based upon the well known approximation of $\beta\sim h/r$. Such an emitter structure is not observed in Fig. 2 where an upper emitter length of 25 μm can be seen giving rise to an enhancement factor of 250. We are able to eliminate space-charge limited current (SCLC) effects since the magnitude of the current in Fig. 3(a) is only 6×10^{-7} A. Furthermore, in the high current regime the current is observed, as shown in the inset of Fig. 3(a), to follow a power law dependence on voltage (field), $I\propto V^n$, with $n=3.0$. While a high value of $n=2.5$ was reported for the saturated current density by Rupesinghe *et al.*[23] and attributed to electron beam interaction from neighboring emitters and hence the onset of a space charge saturation, the level of current in that study was much larger than that observed. The value of n found in the present study is also significantly different from $n=1.5$ or $n=2$ corresponding to a SCLC in either vacuum or in a thin film semiconductor.[24] We believe that the electron emission from the structure at the low applied field was primarily from the nanofiber structures as the surrounding amorphous carbon film has a much higher threshold field of approximately 20 V/μm. It is also possible that the nano-scale dielectric inhomogeneities present close to the carbon nanofibers could help to increase the observed enhancement factor.[25]

V. CONCLUSIONS

In conclusion, carbon nanofibers were grown by plasma enhanced chemical vapor deposition of CH_4 at room temperature on Ni catalyst on glass substrates. The observed structures displayed excellent electron field emission with a low threshold field of 5 V/μm. A Fowler–Nordheim analysis gives rise to an apparently high field enhancement factor of about 4200. However, we believe that the emission of electrons at low fields is due to field enhancement at the tip, but at higher currents the emission becomes bulk limited. We have also shown that it is possible to produce nanostructured Ni films using plasma ion treatment to act as a catalyst material and that the emission is not from the surrounding amorphous carbon.

ACKNOWLEDGMENTS

The authors would like to thank the EPSRC Portfolio Partnership and Carbon Based Electronics programmes for funding this research.

[1] S. Iijima, Nature (London) **56**, 354 (1991).
[2] A. G. Rinzler, J. H. Hafner, P. Nikolaev, L. Lou, S. G. Kim, D. Tománek, P. Nordlander, D. T. Colbert, and R. E. Smalley, Science **269**, 1550 (1995).
[3] J. M. Bonard, H. Kind, T. Stockli, and L. A. Nilsson, Solid-State Electron. **45**, 893 (2001).
[4] I. Alexandrou, E. Kymakis, and G. A. J. Amaratunga, Appl. Phys. Lett. **80**, 1435 (2002).
[5] C. H. Poa, S. R. P. Silva, P. C. P. Watts, W. K. Hsu, H. W. Kroto, and D. R. M. Walton, Appl. Phys. Lett. **80**, 3189 (2002).
[6] K. W. Wong, X. T. Zhou, F. C. K. Au, K. L. Lai, C. S. Lee, and S. T. Lee, Appl. Phys. Lett. **75**, 2918 (1999).
[7] Y. B. Li, Y. Bando, D. Golberg, and K. Kurashima, Appl. Phys. Lett. **81**, 5048 (2002).
[8] Y.-H. Lee, C.-H. Choi, Y.-T. Jang, E.-K. Kim, and B.-K. Ju, Appl. Phys. Lett. **81**, 745 (2002).
[9] J. Chen, S. Z. Deng, and N. S. Xu, Appl. Phys. Lett. **80**, 3620 (2002).
[10] B. O. Boskovic, V. Stolojan, R. U. A. Khan, S. Haq, and S. R. P. Silva, Nat. Mater. **1**, 165 (2002).
[11] S. Hofmann, C. Ducati, B. Kleinsorge, and J. Robertson, New J. Phys. **5**, 153 (2003).
[12] O. A. Louchev, Y. Sato, and H. Kanda, Appl. Phys. Lett. **80**, 2752 (2002).
[13] C. Bower, O. Zhou, W. Zhu, D. J. Werder, and S. Jin, Appl. Phys. Lett. **77**, 2767 (2000).
[14] J. D. Carey, L. L. Ong, and S. R. P. Silva, Nanotechnology **14**, 1223 (2003).
[15] J. D. Carey and S. R. P. Silva, Appl. Phys. Lett. **78**, 347 (2001).
[16] See, for example, *Ion Bombardment Modification of Surfaces: Fundamentals and Applications*, edited by O. Auciello and R. Kelly (Elsevier, Netherlands, 1984).
[17] J. V. Anguita, S. R. P. Silva, and W. Young, J. Appl. Phys. **88**, 5175 (2000).
[18] V. I. Merkulov, D. H. Lowndes, Y. Y. Wei, G. Eres, and E. Voelkl, Appl. Phys. Lett. **76**, 3555 (2000).
[19] See for example, W. Zhu, *Vacuum Microelectronics* (Wiley, New York, 2001).
[20] J.-M. Bonard, K. A. Dean, B. F. Coll, and C. Klinke, Phys. Rev. Lett. **89**, 197602 (2002).
[21] J.-M. Bonard, M. Croci, I. Arfaoui, O. Noury, D. Sarangi, and A. Chatelain, Diamond Relat. Mater. **11**, 763 (2002).
[22] J. B. Cui, K. B. K. Teo, J. T. J. Tsai, J. Robertson, and W. I. Milne, Appl. Phys. Lett. **77**, 1831 (2000).
[23] N. L. Rupesinghe, M. Chhowalla, K. B. K. Teo, and G. A. J. Amaratunga, J. Vac. Sci. Technol. B **21**, 338 (2003).
[24] D. R. Lamb, *Electrical Conduction Mechanism in Thin Insulating Films* (Methuen and Co. Ltd., 1967).
[25] J. D. Carey, R. D. Forrest, and S. R. P. Silva, Appl. Phys. Lett. **78**, 2339 (2001).